JOC Featured Article

pubs.acs.org/joc

Accurate Oxidation Potentials of Benzene and Biphenyl Derivatives via Electron-Transfer Equilibria and Transient Kinetics

Paul B. Merkel,* Pu Luo, Joseph P. Dinnocenzo,* and Samir Farid*

Department of Chemistry and the Center for Photoinduced Charge Transfer, University of Rochester, Rochester, New York 14627-0216

pmerkel@rochester.rr.com; jpd@chem.rochester.edu; farid@chem.rochester.edu

Received May 27, 2009

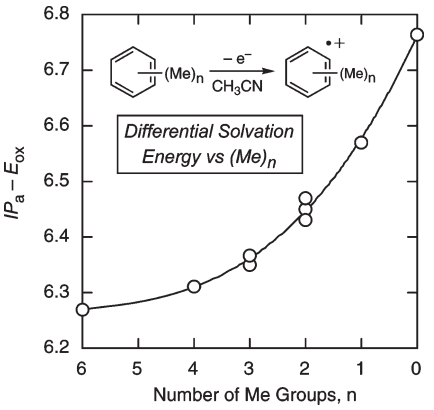

Nanosecond transient absorption methods were used to determine accurate oxidation potentials (E_{ox}) in acetonitrile for benzene and a number of its alkyl-substituted derivatives. E_{ox} values were obtained from a combination of equilibrium electron-transfer measurements and electron-transfer kinetics of radical cations produced from pairs of benzene and biphenyl derivatives, with one member of the pair acting as a reference. Using a redox-ladder approach, thermodynamic oxidation potentials were determined for 21 benzene and biphenyl derivatives. Of particular interest, E_{ox} values of 2.48 ± 0.03 and 2.26 ± 0.02 V vs SCE were obtained for benzene and toluene, respectively. Because of a significant increase in solvent stabilization of the radical cations with decreasing alkyl substitution, the difference between ionization and oxidation potentials of benzene is ~0.5 eV larger than that of hexamethylbenzene. Oxidation potentials of the biphenyl derivatives show an excellent correlation with substituent σ^+ values, which allows E_{ox} predictions for other biphenyl derivatives. Significant dimer radical cation formation was observed in several cases and equilibrium constants for dimerization were determined. Methodologies are described for determining accurate electron-transfer equilibrium constants even when dimer radical cations are formed. Additional equilibrium measurements in trifluoroacetic acid, methylene chloride, and ethyl acetate demonstrated that solvation differences can substantially alter and even reverse relative E_{ox} values.

1. Introduction

Reliable redox potentials for aromatic hydrocarbons are fundamental thermodynamic properties that have a wide range of utility. For example, they are important for developing a detailed understanding of the energetics and kinetics for electron-transfer reactions.[1,2] They are also useful for estimating bond dissociation energies[3] and acidity constants

(1) (a) Beletskaya, I. P.; Makhon'kov, D. I. *Russ. Chem. Rev. (Engl. Transl.)* **1981**, *50*, 534. (b) Chanon, M.; Tobe, M. L *Angew. Chem., Int. Ed. Engl.* **1982**, *21*, 1. (c) Julliard, M.; Chanon, M. *Chem. Rev.* **1983**, *83*, 425.

(2) Gould, I. R.; Ege, D.; Moser, J. E.; Farid, S. *J. Am. Chem. Soc.* **1990**, *112*, 4290.

(3) (a) Okamoto, A.; Snow, M. S.; Arnold, D. R. *Tetrahedron* **1986**, *42*, 6175. (b) Popielarz, R.; Arnold, D. R *J. Am. Chem. Soc.* **1990**, *112*, 3068. (c) Maslak, P.; Vallombroso, T. M.; Chapman, W. H.; Narvaez, J. N. *Angew. Chem., Int. Ed. Engl.* **1994**, *33*, 73. (d) Wayner, D. D.; Parker, V. D. *Acc. Chem. Res.* **1993**, *26*, 287.

DOI: 10.1021/jo9011267 Published on Web 07/09/2009

of radical ions.[3d] In addition, they provide critical benchmark values for testing recent quantum chemical approaches for predicting redox potentials in solution.[4]

For compounds that form reactive radical cations upon one-electron oxidation, the most common cyclic voltammetric (CV) methods for determining oxidation potentials often fail to provide reversible voltammograms. In part for this reason, a wide range of oxidation potentials can frequently be found in the literature. For example, literature oxidation potentials for the fundamental hydrocarbon benzene vary from 2.26 to 2.82 V vs SCE in acetonitrile[5]—a range of nearly 13 kcal/mol! The range of literature oxidation potentials for toluene (1.98−2.40 V) is only marginally better.[5a−c,5k,5m,6] In principle, the use of microelectrodes and fast scan potentiostats[7] allows redox potentials to be measured for radical ions with lifetimes in the nanosecond range.[8] In practice, slow heterogeneous electron transfer at the electrode for molecules like benzene and toluene do not permit the full advantage of fast scan CV techniques to be realized.

Herein, we utilize nanosecond transient absorption spectroscopy to monitor the electron-transfer equilibrium[9,10] established between the radical cation of a reference compound of known oxidation potential and an electron donor of unknown oxidation potential to determine thermodynamically meaningful oxidation potentials for a range of biphenyl (BP) and benzene derivatives (B), including benzene and toluene. The methodology is illustrated for the case in which a BP derivative serves as the reference compound and a B derivative is the compound whose oxidation potential is to be measured by using the redox equilibrium in eq 1, where K_{eq} is the electron-transfer equilibrium constant and k_1 and k_{-1} are the forward and reverse electron-transfer rate constants, respectively. Under conditions where the decay of $B^{\bullet+}$ and $BP^{\bullet+}$ are slow relative to k_1[BP] and k_{-1}[B], an equilibrium is effectively established (see the Supporting Information) involving the radical cations and their unoxidized forms. The difference in the oxidation potentials of BP and B, $E_{ox}(BP) - E_{ox}(B)$, can be determined from eq 2. This analysis makes the conventional assumption that concentrations can be used in place of activity coefficients. Thus, the ΔE_{ox} values derived from the redox equilibrium measurements are strictly differences in formal potentials, rather than standard potentials. We note, however, that the neglect of activity coefficients should be inconsequential in the examples studied herein because the ionic strength of the medium is particularly low (~1 mM) and because the activity coefficients of the species on both sides of the equilibrium in eq 1a are expected to be quite similar.

$$BP + B^{\bullet+} \underset{k_{-1}}{\overset{k_1}{\rightleftharpoons}} BP^{\bullet+} + B \quad (1a)$$

$$K_{eq} = k_1/k_{-1} \quad (1b)$$

$$E_{ox}(BP) - E_{ox}(B) = -RT \ln K_{eq} = -0.0255 \ln K_{eq} \quad (2)$$

Although the redox equilibrium method has the virtue that it can provide oxidation potentials with extraordinary accuracy and precision, it also has some limitations. First, as mentioned above, the method requires that the decay of intermediate radical cations be slow relative to the electron exchange in eq 1a. Second, reliable equilibrium constants can only be determined for donor and reference compounds whose oxidation potentials are relatively similar. For example, a ΔE_{ox} of only 200 mV corresponds to $K_{eq} > 2000$, which is generally too difficult to accurately determine. As we will show, when these conditions are not met the electron-transfer equilibrium constant can instead be reliably determined by kinetic approaches that directly measure the rate constants for electron exchange (k_1 and k_{-1}).[11]

2. Results

We begin by describing the spectral characterization of benzene and biphenyl radical cations in terms of their extinction coefficients at their absorption maxima (λ_{max}). The spectral data are then used to determine ΔE_{ox} for electron-transfer equilibria between different electron donors and their radical cations. Finally, for cases where the equilibrium method is difficult to apply, transient kinetics are used to determine the individual rate constants for electron-transfer equilibration and, thereby, K_{eq} and ΔE_{ox} values.

2.1. Radical Cation Spectra and Extinction Coefficients. Radical cation extinction coefficients ($\varepsilon^{\bullet+}$) were obtained for most electron donors by comparing transient absorption spectra obtained by pulsed laser (7 ns, 343 nm) irradiation of air-saturated acetonitrile solutions containing 1 mM *N*-methylquinolinium hexafluorophosphate (NMQ^+), toluene (0.5 M), and either a BP or a B derivative (~10 mM).

(4) For recent attempts to calculate oxidation potentials, see: (a) Winget, P.; Weber, E. J.; Cramer, C. J.; Truhlar, D. G. *Phys. Chem. Chem. Phys.* **2000**, *2*, 1231. (b) Baik, M.-H.; Friesner, R. A. *J. Phys. Chem. A* **2002**, *106*, 7407. (c) Han, Y.-K.; Jung, J.; Cho, J.-J.; Kim, H.-J. *Chem. Phys. Lett.* **2003**, *368*, 601. (d) Fu, Y.; Liu, L.; Yu, H.-Z.; Wang, Y.-M.; Guo, Q.-X. *J. Am. Chem. Soc.* **2005**, *127*, 7227. (e) Yu, A.; Liu, Y.; Li, Z.; Cheng, J.-P. *J. Phys. Chem. A* **2007**, *111*, 9978. (f) Singh, N. K.; Shaik, M. S.; O'Malley, P. J.; Popelier, P. L. A. *Org. Biomol. Chem.* **2007**, *5*, 1739. (g) Riahi, S.; Norouzi, P.; Bayandori Moghaddam, A.; Ganjali, M. R.; Karimipour, G. R.; Sharghi, H. *Chem. Phys.* **2007**, *337*, 33. (h) Alizadeh, K.; Seyyedi, S.; Shamsipur, M. *Pol. J. Chem.* **2008**, *82*, 1449.

(5) (a) Lund, H. *Acta Chem. Scand.* **1957**, *11*, 1323. (b) Loveland, J. W.; Dimeler, G. R. *Anal. Chem.* **1961**, *33*, 1196. (c) Pysh, E. S.; Yang, N. C. *J. Am. Chem. Soc.* **1963**, *85*, 2124. (d) Neikam, W. C.; Desmond, M. M. *J. Am. Chem. Soc.* **1964**, *86*, 4811. (e) Gough, T. A.; Peover, M. E. *Proceedings of the 3rd International Polarography Congress*, Southhampton, 1965; Macmillan: London, 1966; p 1017. (f) Hansen, R. L.; Toren, P. E.; Young, R. H. *J. Phys. Chem.* **1966**, *70*, 1653. (g) Hoytink, G. J. *Disc. Faraday Soc.* **1968**, *45*, 14. (h) Osa, T.; Yildiz, A.; Kuwana, T. *J. Am. Chem. Soc.* **1969**, *91*, 3994. (i) Parker, V. D. *J. Am. Chem. Soc.* **1976**, *98*, 98. (j) Tanimoto, I.; Kushioka, K.; Kitagawa, T.; Maruyama, K. *Bull. Chem. Soc. Jpn.* **1979**, *52*, 3586. (k) Howell, J. O.; Goncalves, J. M.; Amatore, C.; Klasinc, L.; Wightman, R. M.; Kochi, J. K. *J. Am. Chem. Soc.* **1984**, *106*, 3968. (l) Butin, K. P.; Moiseeva, A. A.; Magdesieva, T. V.; Sergeeva, E. V.; Rozenberg, V. I.; Kharitonov, V. G. *Russ. Chem. Bull.* **1994**, *43*, 783. (m) Fukuzumi, S.; Ohkubo, K.; Suenobu, T.; Kato, K.; Fujitsuka, M.; Ito, O. *J. Am. Chem. Soc.* **2001**, *123*, 8459.

(6) Neikam, W. C.; Dimeler, G. R.; Desmond, M. M. *J. Electrochem. Soc.* **1964**, *111*, 1190.

(7) (a) Wightman, R. M.; Wipf, D. O. *Electroanal. Chem.* **1989**, *15*, 267. (b) Andrieux, C. P.; Hapiot, P.; Saveant, J.-M. *Chem. Rev.* **1990**, *90*, 723. (c) Heinze, J. *Angew. Chem., Int. Ed. Engl.* **1993**, *32*, 1268. (d) Amatore, C.; Bouret, Y.; Maisonhaute, E.; Abruna, H. D.; Goldsmith, J. I. *C. R. Chim.* **2003**, *6*, 99.

(8) Amatore, C.; Maisonhaute, E.; Simmoneau, G. *J. Electroanal. Chem.* **2000**, *486*, 141.

(9) For reviews, see: (a) Steenken, S. *Landolt-Börnstein* **1985**, *13e*, 147. (b) Wardman, P. *J. Phys. Chem. Ref. Data* **1989**, *18*, 1637. (c) Stanbury, D. M. In *General Aspects of the Chemistry of Radicals*; Alfassi, Z. B., Ed.; Wiley: New York, 1999; Chapter 11.

(10) Guirado, G.; Fleming, C. N.; Lingenfelter, T. G.; Williams, M. L.; Zuilhof, H.; Dinnocenzo, J. P. *J. Am. Chem. Soc.* **2004**, *126*, 14086.

(11) Gould, I. R.; Wosinska, Z. M.; Farid, S. *Photochem. Photobiol.* **2006**, *82*, 104.

Although this system for generating radical cation spectra has been described in detail elsewhere,[10] we highlight its essential features here for clarity. Pulsed laser excitation of NMQ^+ produces its singlet-excited state ($^1NMQ^{+}*$), which is rapidly intercepted by toluene to efficiently produce toluene$^{\bullet+}$ and the *N*-methylquinolinyl radical ($NMQ^{\bullet}$) by photoinduced electron transfer. $NMQ^{\bullet}$ is rapidly scavenged by dioxygen in <200 ns leading to $O_2^{\bullet-}$, which does not have interfering absorptions in the visible region where the radical cations strongly absorb. Interception of toluene$^{\bullet+}$ by the BP or B derivatives produces their radical ions with a concentration essentially independent of the donor. At the moderate laser powers used in these experiments there was typically minimal second-order decay of the radical ions at 200 ns, such that the transient spectral maxima provided a direct measure of the *relative* extinction coefficients of the $BP^{\bullet+}$ and $B^{\bullet+}$ derivatives. Absolute extinction coefficients were determined by using biphenyl radical cation ($BP6^{\bullet+}$) as reference ($\varepsilon^{\bullet+} = 14500\ M^{-1}\ cm^{-1}$ at 668 nm in acetonitrile).[2]

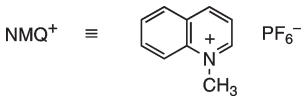

The method for determining radical cation extinction coefficients described above is suitable only for electron donors whose oxidation potentials are significantly lower than that of toluene. For donors with E_{ox} values close to or greater than that of toluene, $\varepsilon^{\bullet+}$ values were obtained without toluene by comparing transient absorption spectra of solutions with sufficient concentration of B or BP to efficiently quench $^1NMQ^{+}*$. Repetition of these experiments in the presence of a low concentration of biphenyl ($\sim$1 mM) permitted conversion of $B^{\bullet+}$ or $BP^{\bullet+}$ to biphenyl$^{\bullet+}$ prior to significant radical cation decay. The absolute $\varepsilon^{\bullet+}$ values of $B^{\bullet+}$ and $BP^{\bullet+}$ could then be determined from the known $\varepsilon^{\bullet+}$ for biphenyl$^{\bullet+}$, as described above. Typical radical cation absorption spectra are shown in Figure 1. A summary of the extinction coefficients and spectral maxima for all of the radical cations studied are provided in the second and third columns of Table 1.

2.2. Dimer Radical Cation Formation. During the course of our experiments, we noted that the radical cation equilibria for some of the benzene derivatives were complicated by the formation of dimer radical cations[12] ($B_2^{\bullet+}$) when the neutrals were used in high ($\geq$0.05 M) concentrations. At these concentrations, the equilibration in eq 3 must be taken into account for the accurate determination of E_{ox} values.

$$B + B^{\bullet+} \overset{K_D}{\rightleftharpoons} B_2^{\bullet+} \qquad (3)$$

It was possible to obtain the equilibrium constant (K_D) for $B_2^{\bullet+}$ formation from measurements of transient absorption spectra of the donor radical cations as a function of donor concentration. For example, shown in Figure 2 are the spectral changes for solutions containing toluene radical cation as a function of toluene concentration. These spectra

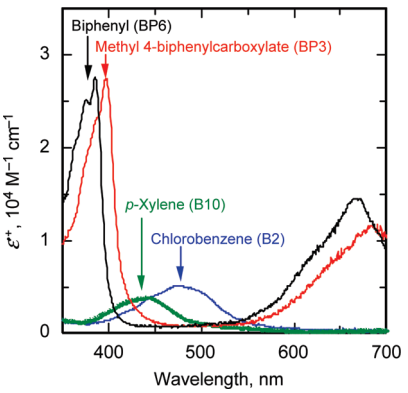

FIGURE 1. Radical cation absorption spectra of biphenyl (BP6), methyl 4-biphenylcarboxylate (BP3), *p*-xylene (B10), and chlorobenzene (B2) generated by laser pulse excitation (7 ns, 343 nm) of 0.01 M solutions of donor (except 0.1 M for B2) with 1 mM NMQ^+ in air-saturated acetonitrile. Solutions of BP3, BP6, and B10 also contained 0.5 M toluene codonor.

were generated by pulsed laser excitation of air-saturated acetonitrile solutions of NMQ^+ containing 0.05−2.0 M toluene. Following reaction of $NMQ^{\bullet}$ with O_2, the radical cations $B^{\bullet+}$ and $B_2^{\bullet+}$ are the only species that absorb in the visible region of the transient absorption spectra. The increases in optical density that occur at wavelengths >600 nm with higher concentrations of toluene reflect the formation of $B_2^{\bullet+}$.[12] At these wavelengths essentially only $B_2^{\bullet+}$ absorbs. The absorption spectra of $B^{\bullet+}$ and $B_2^{\bullet+}$ are similar near 430 nm, and the extinction coefficients of the two species are nearly the same in this region. By fitting the changes in the absorption at 750 nm to the expression $[B_2^{\bullet+}]/[B^{\bullet+}] = K_D[B]$, which assumes negligible $B^{\bullet+}$ absorption at this wavelength, a K_D value of 5 was determined for toluene in acetonitrile. K_D values for five other benzene derivatives that formed dimer radical cations were determined in a similar manner (Table 2). Negligible radical cation dimerization was observed for the other benzene derivatives or for any of the biphenyl derivatives used in this study.

When toluene was used as a codonor at high concentrations, spectral evidence was found for complex formation between toluene and the radical cations of three benzene derivatives (toluene/$B^{\bullet+}$) according to eq 4. Estimates for the mixed complex formation constants (K_C) were determined in an analogous manner to the K_D values and are listed in Table 2.

$$\text{toluene} + B^{\bullet+} \overset{K_C}{\rightleftharpoons} \text{toluene}/B^{\bullet+} \qquad (4)$$

Fortunately, the magnitudes of the K_D and K_C values in Table 2 are small enough that equilibria (3) and (4) do not significantly interfere with the determination of equilibrium oxidation potentials for the vast majority of substrates studied here. As will be shown, only in the case of electron-transfer equilibria involving benzene did dimer radical cation formation need to be explicitly considered for the determination of accurate oxidation potentials.

2.3. E_{ox} Values via Radical Cation Equilibria. E_{ox} values were obtained by measuring electron-transfer equilibrium constants of reaction 1a for each benzene derivative (B1−B13) vs one or more biphenyl derivatives (BP1−BP8). A redox ladder was created with these compounds using

(12) Bockman, T. M.; Karpinski, Z. J.; Sankararaman, S.; Kochi, J. K. *J. Am. Chem. Soc.* **1992**, *114*, 1970.

TABLE 1. Radical Cation Spectral Data and Oxidation Potentials of Benzene and Biphenyl Derivatives in Acetonitrile

	donor	$\varepsilon^{\bullet+}$ (M^{-1} cm^{-1})	λ_{max} (nm)	E_{ox} (V vs SCE)
	benzene derivatives[a]			
B1	benzene	2200	432	2.48 ± 0.03
B2	chlorobenzene	5100	473	2.46 ± 0.03
B3	*tert*-butylbenzene	2900	448	2.28 ± 0.02
B4	toluene	2900	429	2.26 ± 0.02
B5	*m*-xylene	3200	448	2.10 ± 0.01
B6	*o*-xylene	2800	431	2.09 ± 0.01
B7	1,4-di-*tert*-butylbenzene	4700	470	2.06 ± 0.01
B8	mesitylene	3200	475	2.05 ± 0.01
B9	1,3,5-tri-*tert*-butylbenzene	3800	498	2.04 ± 0.01
B10	*p*-xylene	3900	437	2.01 ± 0.01
B11	1,2,4-trimethylbenzene	4000	447	1.905 ± 0.01
B12	1,2,3,4-tetramethylbenzene	3300	460	1.825 ± 0.01
B13	1,2,3,5-tetramethylbenzene	3750	464	1.82 ± 0.01
B14	durene	4900	454	1.75[b]
	biphenyl derivatives			
BP1	4-CO_2Bu, 4′-CF_3	13800, 33500	692, 394	2.35 ± 0.02
BP2	4-CO_2Bu, 4′-CO_2Bu	14500, 42200	708, 406	2.28 ± 0.02
BP3	4-CO_2Me	11500, 28000	682, 395	2.10 ± 0.01
BP4	3-CO_2H	12700, 25300	666, 385	2.06 ± 0.01
BP5	4-Br, 4′-Br	11000, 37000	704, 423	1.98 ± 0.01
BP6	biphenyl	14500,[c] 28000	668, 383	1.95[d]
BP7	4-OCOMe	15200, 31000	672, 399	1.81 ± 0.01
BP8	4-Me	14400, 32300	670, 393	1.795 ± 0.01

[a]For comparison, reversible oxidation potentials in acetonitrile have been reported for other methyl-substituted benzenes: pentamethylbenzene (1.69) and hexamethylbenzene (1.58 V vs SCE), respectively.[13] [b]From ref 13. [c]From ref 2. [d]From ref 10.

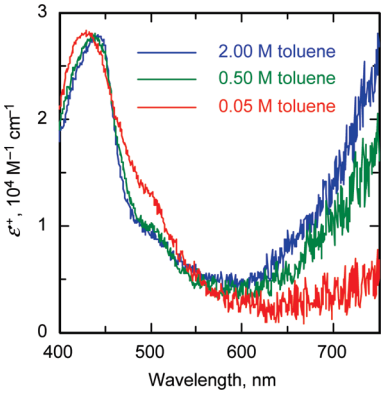

FIGURE 2. Transient radical cation absorption spectra (molar absorptivity units) measured 300 ns after 343 nm laser excitation of air-saturated acetonitrile solutions containing 1 mM NMQ^+ and 0.05, 0.50, and 2.0 M toluene.

biphenyl (BP6) and durene (B14) as redox anchors. The oxidation potential of BP6 was previously determined from redox equilibration experiments[10] and, in turn, rests on the carefully measured value for E_{ox}(B14) determined by Amatore and Lefrou using ultrafast scan cyclic voltammetry and ultramicroelectrodes.[13] Appropriate concentrations of donors were used so that equilibration among donors and their radical cations was much faster than radical ion decay, which typically required several microseconds, thus allowing an equilibrium to be effectively established in solutions containing the two electron-donors.

The electron-transfer equilibrium constants (K_{eq}) were calculated from $[BP][B^{\bullet+}]/[B][BP^{\bullet+}]$, and ΔE_{ox} was calculated from eq 2. At low pulse energies, the concentrations of the radical cations ($\leq 10^{-5}$ M) are very small compared to those of the neutral species [B] and [BP], which are indistinguishable from the initial concentrations. The low concentrations of radical cations render potential bimolecular coupling reactions insignificant relative to their first-order decay, which proceeds with a rate constant of $\sim 2 \times 10^5$ s^{-1} (vide infra). Although absolute radical cation extinction coefficients are provided in Table 1, the determinations of K_{eq} depends only on relative extinction coefficients, which were determined with higher precision (5−10%) in the equilibration experiments. It is worth noting that even an uncertainty of 10% in the relative extinction coefficients corresponds to an error in ΔE_{ox} of only 0.002 V. In general, transient absorption spectra were obtained at successive delay times to ascertain that the ratio of absorptions of $B^{\bullet+}$ and $BP^{\bullet+}$ remained constant and that equilibrium was achieved.

TABLE 2. Equilibrium Constants for Radical Cation Dimerization, K_D, and for Complexation with Toluene, K_C, in Acetonitrile at Ambient Temperature

benzene derivative	K_D (M^{-1})[a]	K_C (M^{-1} toluene)[a]
benzene	12	
tert-butylbenzene	2	
toluene	5	
m-xylene	5	2
o-xylene	4	1.5
p-xylene	2	0.5

[a]Estimated error, ~20%.

Typical equilibrium spectra are illustrated in Figure 3 for biphenyl (BP6) and *p*-xylene (B10). Spectra of $BP6^{\bullet+}$ and $B10^{\bullet+}$ are given by traces a and b, respectively. Experimentally measured equilibrium mixtures of the two radical cation species at two different donor concentrations are shown in spectra c and d. These spectra can be fit quite well by appropriate combinations of the pure radical cation spectra a and b, as shown by plots e and f. The ratios of the radical cations comprising plots e and f together with the associated concentrations of BP6 and B10 provide an experimental equilibrium constant (K_{eq}) of 11−12. This yields

(13) Amatore, C.; Lefrou, C. *J. Electroanal. Chem.* **1992**, *325*, 239.

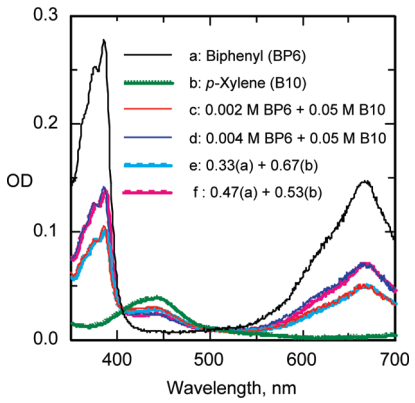

FIGURE 3. Transient radical cation absorption spectra measured 500 ns after 343 nm laser excitation of air-saturated acetonitrile solutions containing 1 mM NMQ^+ and 0.5 M toluene with (a) 0.01 M biphenyl (BP6), (b) 0.05 M *p*-xylene (B10), (c) 0.002 M BP6 + 0.05 M B10, and (d) 0.004 M BP6 + 0.05 M B10. Curve (e) is a fit of (c) with 33% of (a) plus 67% of (b), and curve (f) is a fit of (d) with 47% of (a) plus 53% of (b), which yield $K_{eq} = 11-12$ for eq 1 and ΔE_{ox} (BP6 − B10) = −0.06 V.

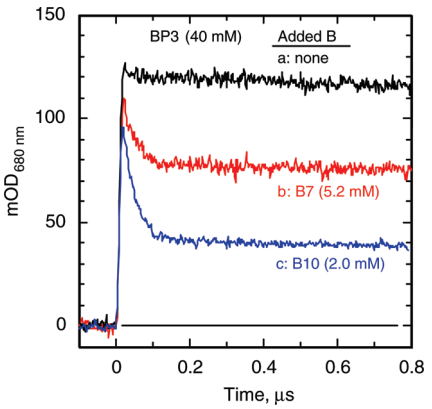

FIGURE 4. Transient absorption of the radical cation of methyl 4-biphenylcarboxylate, BP3, monitored at 680 nm, as a function of time, following 343 nm laser excitation of air-saturated acetonitrile solutions containing 1 mM NMQ^+ and 40 mM BP3 with (a) no added donor, (b) 2.6 mM 1,4-di-*tert*-butylbenzene (B7), and (c) 2 mM *p*-xylene (B10). Trifluoroacetic anhydride (0.04 M) was added to scavenge traces of water in acetonitrile and increase the radical cation lifetimes for these experiments.

ΔE_{ox} (BP6 − B10) of −0.06 V which, coupled with E_{ox}(BP6) = 1.95, gives E_{ox}(B10) = 2.01 vs SCE. Analogous experiments were performed with different concentrations of BP6 and B10 without toluene as a codonor. In all cases, the E_{ox} value for B10 was 2.01 V vs SCE within experimental error (±0.01 V). These latter experiments demonstrate that the toluene/*p*-xylene$^{\bullet+}$ complex described above does not detectably affect the determination of the electron-transfer equilibrium constant.

Additional examples of the determination of E_{ox} values by the fitting of full radical cation spectra of pairs of donors under equilibrium conditions are provided in the Supporting Information. While this method has the advantage that the entire radical cation spectra are used to determine E_{ox}, equally accurate values could be obtained from the ratio (R) of optical densities of pairs of radical cations in equilibrium at two wavelengths, a and b, according to eqs 5a and 5b[14,15] Ideally, the wavelengths are chosen to yield minimal values (preferably zero) for the extinction coefficient ratios y and z. As illustrated by the spectra in Figures 1 and 3, donor pairs consisting of a biphenyl derivative (BP) and a benzene derivative (B) are particularly well suited to such determinations due to the large differences in their radical cation absorption maxima. Because the radical cations of all BP derivatives have two prominent absorption peaks (Figure 1), K_{eq} and E_{ox} values were determined using each of the BP absorption maxima as wavelength a in the above calculations to provide a check on calculated values. In general, the E_{ox} values obtained using the two different $BP^{\bullet+}$ absorption maxima agreed to within 0.005 V.

$$R = (OD^a/OD^b) \tag{5a}$$

$$\frac{[B^{\bullet+}]}{[BP^{\bullet+}]} = \frac{x - yR}{R - z} \tag{5b}$$

where

$$x = \frac{(\varepsilon_{BP^{\bullet+}})^a}{(\varepsilon_{B^{\bullet+}})^b} \quad y = \frac{(\varepsilon_{BP^{\bullet+}})^b}{(\varepsilon_{B^{\bullet+}})^b} \quad z = \frac{(\varepsilon_{B^{\bullet+}})^a}{(\varepsilon_{B^{\bullet+}})^b}$$

In some cases, it was also possible to measure K_{eq} and E_{ox} values by comparing transient absorption spectra of two different BP derivatives or two B derivatives, providing that their radical cation spectra were sufficiently different. One example is the pair consisting of BP5 and BP6, for which the absorption maximum of the strong radical cation bands in the near UV and blue are 423 and 383 nm, respectively. From the equilibration of BP5 and BP6 and their radical cations a ΔE_{ox}(BP5 − BP6) of 0.03 V was obtained.

In several cases, both the full spectrum fitting and the two-wavelength methods were used to determine E_{ox} values. When this was done, the agreement between the methods was excellent. Oxidation potentials vs SCE in acetonitrile at 295 K obtained by one or both of these methods are provided in the last column of Table 1. In many cases, more than one reference donor was used to obtain E_{ox} of the target donor (see the Supporting Information for a detailed redox ladder). As expected, the error estimates in E_{ox} naturally increase the further removed they are from the redox anchors, BP6 and B14, due to propagation of errors.

As also shown in Table 1, *tert*-butylbenzene and 1,4-di-*tert*-butylbenzene were found to have slightly *higher* oxidation potentials in acetonitrile than their methyl-substituted analogues toluene and *p*-xylene. Interestingly, literature oxidation potentials determined by cyclic voltammetry (CV) at slow scan rate in CH_3CN and at high scan rate (200−2000 V/s) in CF_3CO_2H show the opposite trend in E_{ox} values.[5k] That the *tert*-butyl-substituted benzene derivatives have higher oxidation potentials in CH_3CN is additionally confirmed for 1,4-di-*tert*-butylbenzene (B7) vs *p*-xylene (B10) by the data shown in Figure 4. In this experiment, $BP3^{\bullet+}$ is generated and allowed to undergo equilibration with added B7 or B10 by monitoring the absorption of $BP3^{\bullet+}$ at 680 nm, where the benzene radical cations do not absorb. Shown in trace a is the absorbance of $BP3^{\bullet+}$ with no

(14) Meisel, D.; Neta, P. *J. Am. Chem. Soc.* **1975**, *97*, 5198.
(15) For an analogous approach used for equilibration between two excited triplet states, see: Merkel, P. B.; Dinnocenzo, J. P. *J. Photochem. and Photobiol. A, Chem.* **2008**, *193*, 110.

added donor. When 2.6 mM of B7 is added (trace b), the initial absorbance of $BP3^{\bullet+}$ rapidly decreases, with consequent formation of $B7^{\bullet+}$, until equilibrium is reached after ~0.2 μs. Importantly, addition of a lower concentration (2.0 mM) of *p*-xylene (B10) leads to a *larger* decrease in the absorption of $BP3^{\bullet+}$, indicating a greater formation of $B10^{\bullet+}$. These data clearly demonstrate that $E_{ox}(B7) > E_{ox}(B10)$. A quantitative analysis gives equilibrium constants of 5 ± 0.7 for B7/BP3 and of 39 for B10/BP3, which correspond to an oxidation potential for B7 that is 0.05 V higher than B10 in acetonitrile.

To determine if differential solvation could substantially alter relative oxidation potentials, analogous experiments were performed with BP3, B7, and B10 in trifluoroacetic acid containing 7 vol % trifluoroacetic anhydride—the same solvent system used in previous fast scan CV experiments.[5k] Interestingly, we found that trifluoracetic acid indeed alters the relative oxidation potentials of B7 and B10, with B7 being *easier* to oxidize than B10 by 0.02 V in CF_3CO_2H, which agrees well with that obtained by fast scan CV (0.03 V). Additional comparative equilibration experiments with B7, B10, and BP3 were carried out in methylene chloride and in ethyl acetate. It was found that the E_{ox} of B7 is 0.01 V higher than that of B10 in methylene chloride and 0.06 V higher in ethyl acetate, which underscores the need to consider varying solvation effects when comparing oxidation potential data.

2.4. E_{ox} Values via Electron-Transfer Kinetics. The redox equilibrium method described above is not suitable for the determination of accurate oxidation potentials when the oxidation potential difference between two compounds is large and/or the decay of their radical cations is competitive with the electron exchange process. In these cases, the electron-transfer equilibrium constants can instead be conveniently determined by transient kinetics.[11] As we will show, kinetic methods can also be successfully applied to reactions where dimer radical cation formation (eq 3) affects the electron-transfer equilibrium.

We first describe application of kinetic methods for determining K_{eq} using the simplified kinetic analysis shown in Scheme 1, where the decay rate constants for the radical cations k_d and k'_d are included in the analysis and dimer radical cation formation is unimportant. The forward and reverse electron-transfer rate constants (k_1 and k_{-1}) that define the electron-transfer equilibrium can be obtained from fitting the changes in optical density (ΔOD) as a function of time (t) according to the well-known kinetic expressions in eq 6.[16]

When $k_d \approx k'_d$ it is easy to show from eq 6c that $\lambda_2 \approx k_d \approx k'_d$ and is, therefore, independent of the concentration ratio of the reactants, B and BP. For the systems described here, we found λ_2 to be nearly constant and first order ($1.8 \pm 0.3 \times 10^5$ s^{-1}) at low laser power, suggesting that decay of the radical cations was primarily through reaction with water or other trace impurities. When $\lambda_2 \approx k_d \approx k'_d$, the difference in time constants, $\lambda_1 - \lambda_2$, is equal to $k_1[BP] + k_{-1}[B]$, to a very good approximation (eq 6f). In practice, the individual values of k_1 and k_{-1} could be obtained via eq 6f from experiments where [B] and [BP] were varied. Because λ_1 was more than an order of magnitude greater than λ_2 small variations in λ_2 had a negligible effect on the determination of λ_1.

SCHEME 1

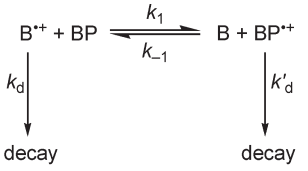

$$\Delta OD = c_1 \exp(-\lambda_1 t) + c_2 \exp(-\lambda_2 t) + c_3 \quad (6a)$$

$$\lambda_1 = 0.5\,(X + Y) + 0.5\,\{(X - Y)^2 + 4k_1[BP]\,k_{-1}[B]\}^{1/2} \quad (6b)$$

$$\lambda_2 = 0.5\,(X + Y) - 0.5\,\{(X - Y)^2 + 4k_1[BP]\,k_{-1}[B]\}^{1/2} \quad (6c)$$

$$X = k_1[BP] + k_d \quad (6d)$$

$$Y = k_{-1}[B] + k'_d \quad (6e)$$

$$\lambda_1 - \lambda_2 \approx k_1[BP] + k_{-1}[B] \quad \text{when } k_d \approx k'_d \quad (6f)$$

In addition to pseudo-first-order decay by reaction with impurities, the decay of radical cations can also occur by return electron transfer (via $O_2^{\bullet-}$ in this case)—a second-order process. This latter contribution was deliberately minimized by use of low laser power. The small, unavoidable contribution from this reaction that remained was approximated[11] as an additional first-order decay. Occasionally, the decay does not completely go to a zero baseline, which was accommodated in the fitting procedure by the constant c_3 in eq 6. In all cases, the contribution from c_3, if any, was < 1% of the maximum optical density.

The kinetic procedure described above utilizes the reaction time constants λ_1 and λ_2 to determine k_1 and k_{-1} and, thereby, the equilibrium constant for electron transfer (K_{eq}). We additionally determined K_{eq} by use of the pre-exponential factor c_1 in eq 6a, which provides a simple relationship between the relative concentrations of the two radical cations. Consider the case of a B/BP system in which B has a higher E_{ox} than that of BP and [B] ≫ [BP]. Under these conditions, the one-electron oxidation of the substrates is initiated almost entirely by interception of the excited sensitizer by B. If the kinetics are monitored at a wavelength where $\varepsilon_{BP^{\bullet+}} > \varepsilon_{B^{\bullet+}}$, a growth in the optical density is observed followed by decay of the radical cations. The relationship between the optical density and equilibrium constant is then given by eq 7, where OD_0 is the optical density at $t = 0$ in the absence of BP, OD_∞ corresponds to the maximum attainable optical density when all initially produced $B^{\bullet+}$ is intercepted by BP to form $BP^{\bullet+}$, and OD is the optical density from the equilibrium mixture of $B^{\bullet+}$ and $BP^{\bullet+}$ in the absence of decay. This OD and OD_∞ are given by c_1, eq 6a. The reciprocal of the slope of a plot of the optical

(16) (a) Birks, J. B. *Photophysics of Aromatic Molecules*; Wiley-Interscience: New York, 1970. (b) Birks, J. B.; Dyson, D. J.; Munro, I. H. *Proc. R. Soc. London* **1963**, *275*, 575.

(17) As defined in the text, the ratio of the optical densities (OD_∞/OD_0) is equal to ratio of the extinction coefficients ($\varepsilon_{BP^{\bullet+}}/\varepsilon_{B^{\bullet+}}$) at the analyzing wavelength. Thus, from this ratio and the experimentally determined OD_0 the nominator in eq 7, ($OD_\infty - OD_0$), can be calculated. Alternatively, and more accurately, (OD_∞/OD_0) is obtained from the reciprocal of the intercept of a plot of $1/(OD - OD_0)$ vs [B]/[BP]. Cf. ref 14.

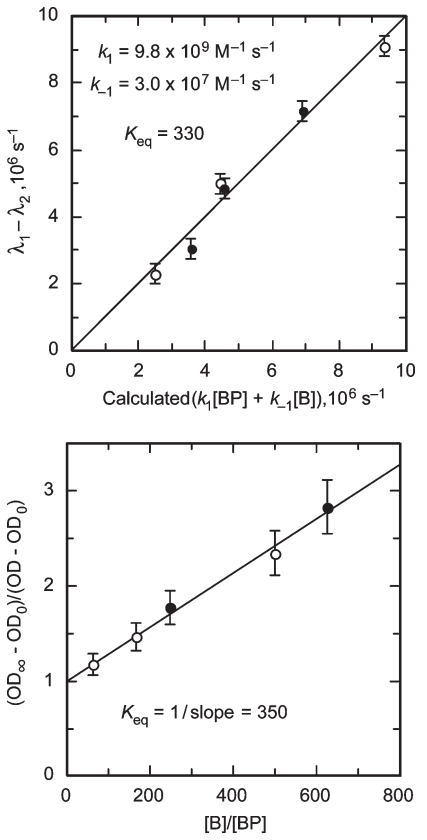

FIGURE 5. Determination of the electron-transfer equilibrium constant involving toluene and methyl 4-biphenylcarboxylate (BP3). The toluene concentration was 0.05 M (unfilled circles) or 0.1 M (filled circles). Top: plot of $(\lambda_1 - \lambda_2)$ (see text) vs the sum of the electron-transfer exchange rates (Scheme 1) using the best-fit rate constants given in the figure. Bottom: plot of the optical density function of eq 7 vs the reactants ratio.

density function of eq 7 vs [B]/[BP] is equal to the equilibrium constant.[17]

$$\frac{OD_\infty - OD_0}{OD - OD_0} = 1 + \frac{1}{K_{eq}}\frac{[B]}{[BP]} \qquad (7)$$

The results from determining the equilibrium constants using both the time constants (λ_1 and λ_2) and the pre-exponential (c_1) methods are illustrated in Figure 5 for the case of toluene (B4) and the biphenyl carboxylate derivative BP3. As shown in Figure 5, the equilibrium constants determined from both kinetic methods are in excellent agreement ($K_{eq} = 330$ and 350, respectively) and correspond to ΔE_{ox} values that differ by < 0.002 V. That good fits are obtained at two different toluene concentrations (0.05 and 0.1 M) demonstrates that the formation of toluene dimer radical cation does not detectably affect the determination of K_{eq}. As described below, this contrasts with experiments to determine the oxidation potential of benzene, where dimer radical cation formation must be taken into account.

The effects of dimer radical cation formation during electron-transfer equilibration can be accounted for by Scheme 2, where the decay rate constants of the radical cations (k_d and k'_d) discussed above are not shown for clarity.

Differences in the electron-transfer rate constants between the monomeric species (k_1 and k_{-1}) and those of the

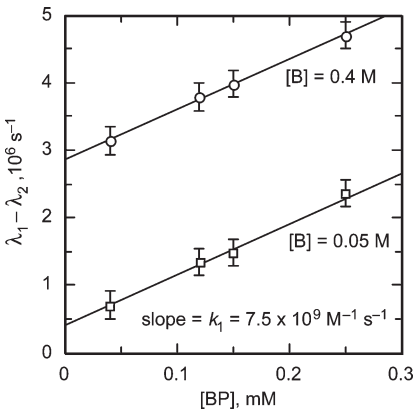

FIGURE 6. Plot of the difference between the time constants $(\lambda_1 - \lambda_2)$, which corresponds to $(k_1[BP] + k_{-2}[B])$, for benzene/BP2 in acetonitrile vs [BP] at two benzene concentrations.

SCHEME 2

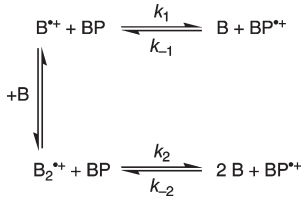

corresponding reactions involving $B_2^{\bullet+}$ (k_2 and k_{-2}) can be obtained from experiments in which [B] is kept constant and [BP] varied and vice versa. This is illustrated in Figure 6 for the equilibrium involving the radical cations of benzene and the biphenyldicarboxylate derivative BP2. As described above, $(\lambda_1 - \lambda_2)$ corresponds to $k_1[BP] + k_{-1}[B]$, here measured at two different concentrations of [B]. Because in each data set [B] was kept constant, the slope of the fitting line is equal to the effective rate constant (weighted average of k_1 and k_2) to form $BP^{\bullet+}$. That the slopes of the fitting lines at [B] = 0.05 and 0.4 M are essentially the same (7.5×10^9 M^{-1} s^{-1}), while the ratio of $B^{\bullet+}/B_2^{\bullet+}$ changes from 62:38 to 17:83, respectively, shows that k_1 must be very similar to k_2. This result is somewhat surprising because the equilibrium constant for dimer formation ($K_D = 12$ M^{-1}, Table 2) indicates that $B_2^{\bullet+}$ is 60 meV lower in energy than $B^{\bullet+}$ + B. Apparently the k_1 and k_2 steps, both being exothermic, are not significantly affected by this difference in driving force.

Next, the concentration of [BP] was held constant and that of [B] was varied, with the data being analyzed using the reaction time constants and the optical densities vs [B] as described above. If there were no reverse electron transfer involving two benzene molecules, i.e., negligible k_{-2}, both plots would be linear, which is clearly not the case (Figure 7). The upward curvature of both plots indicates that the apparent equilibrium constant *decreases* with *increasing* concentration of [B] due to an increasing contribution from k_{-2}.

Both sets of data in Figure 7 were fitted *globally* according to Scheme 2 using $k_1 = k_2 = 7.5 \times 10^9$ M^{-1} s^{-1}, as established from the data shown in Figure 6. Values for the two remaining parameters, k_{-1} and k_{-2}, were varied to obtain the best fits. The curves shown in Figure 7 are based on $k_{-1} = 3.4 \times 10^6$ M^{-1} s^{-1} and $k_{-2} = 1 \times 10^7$ M^{-2} s^{-1}, providing $K_{eq} = k_1/k_{-1} = 2200$ for

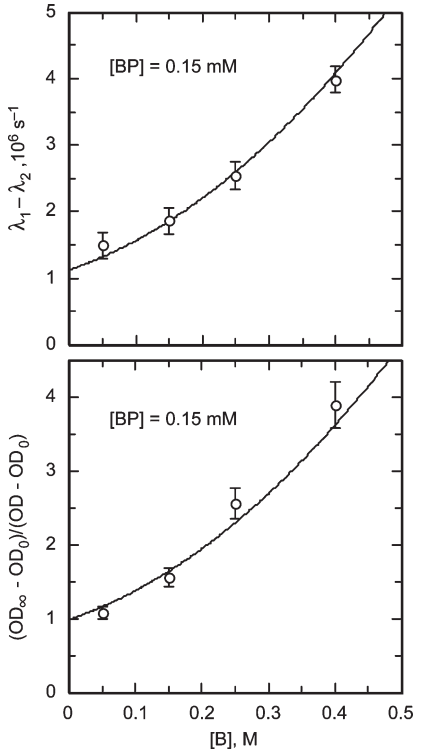

FIGURE 7. Plots of a function of the electron-transfer rates, eq 6f (top), and of the optical densities, eq 7 (bottom), for benzene/BP2 in acetonitrile as a function of benzene concentration at a constant [BP2] of 0.15 mM.

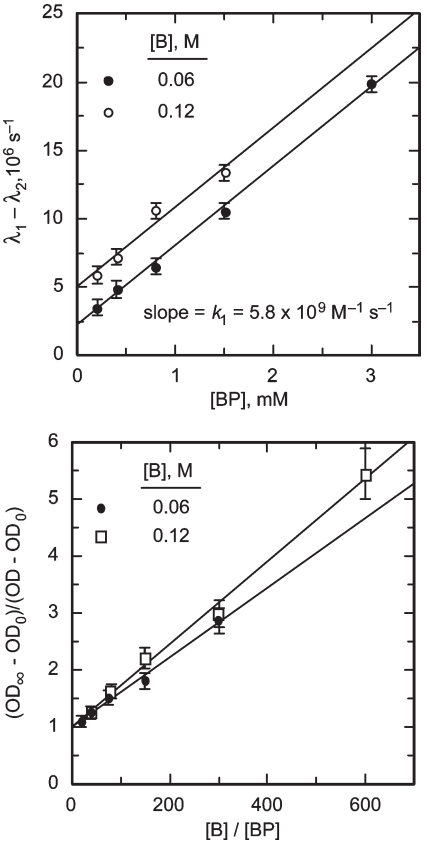

FIGURE 8. Kinetic data for equilibration involving the radical cations of benzene and BP1 in acetonitrile. Top: plot of a function of electron-transfer rates, eq 6f, vs [BP1] at two different concentrations of benzene. Bottom: plot of a function of optical densities, eq 7, vs [benzene]/[BP1].

the benzene/BP2 equilibrium constant. The corresponding value of ΔE_{ox} is 0.20 V, which leads to an oxidation potential for benzene of 2.48 V vs SCE.

We note that the larger value for k_{-2} relative to k_{-1} reflects the lower oxidation potential for $2\,B \rightarrow B_2^{\bullet+}$ than $B \rightarrow B^{\bullet+}$. The one-electron reduction of $BP^{\bullet+}$ by two molecules of B to form $B_2^{\bullet+}$ can be attributed to reaction of a $(BP^{\bullet+}/B)$ cage encounter pair with a second molecule of benzene or to encounters between $BP^{\bullet+}$ and two molecules of B in close proximity.

The equilibrium involving the radical cations of benzene and the biphenyl derivative BP1 was also analyzed using the kinetic approaches described above for the benzene/BP2 system. Because of the smaller E_{ox} gap for the benzene/BP1 pair, the rate constant k_{-1} ($\sim 3.1 \times 10^7\ M^{-1}\ s^{-1}$) is nearly an order of magnitude larger than that of benzene/BP2, which precluded analyses at high benzene concentrations. Nevertheless, as shown in Figure 8, k_1 is still equal to k_2 ($5.8 \times 10^9\ M^{-1}\ s^{-1}$) and k_{-2} affects the equilibrium between the radical cations. The best-fit for benzene/BP1 electron-transfer equilibrium constant is ~190, which leads to ΔE_{ox} = 0.13 V and a benzene oxidation potential of 2.48 V vs SCE. Because of the necessitated limits on data acquisition at high benzene concentrations, k_{-1} was not as well determined as in the benzene/BP2 case. Nonetheless, the oxidation potential of benzene derived from this experiment is identical to that obtained from the benzene/BP2 equilibrations.

3. Discussion

The accurate oxidation potentials provided by this work can be used to critically test a variety of structure−property relationships. For example, numerous attempts have been previously made to correlate the oxidation potentials of substituted benzene derivatives with gas-phase ionization potentials to determine the effects of solvation.[5c,6,18] Using the oxidation potentials in Table 1, such a comparison can now be made with confidence in the reliability of the E_{ox} values. Shown in the top part of Figure 9 is a plot of oxidation potentials for the benzene derivatives in Table 1 vs the corresponding adiabatic ionization potentials (IP_a), where the latter are available.[19] The plot leads to several important conclusions. First, the correlation for benzene and

(18) For representative examples, see: (a) Miller, L. L.; Nordblom, G. D.; Mayeda, E. A. *J. Org. Chem.* **1972**, *37*, 916. (b) Nelsen, S. F.; Peacock, V.; Weisman, G. R. *J. Am. Chem. Soc.* **1976**, *98*, 5269. (c) Loutfy, R. O. *J. Chem. Phys.* **1977**, *66*, 4781. (d) Nelsen, S. F. *Isr. J. Chem.* **1979**, *18*, 45. (e) Gassman, P. G.; Mullins, M. J.; Richtmeier, S.; Dixon, D. A. *J. Am. Chem. Soc.* **1979**, *101*, 5793. (f) Klinger, R. J.; Kochi, J. K. *J. Am. Chem. Soc.* **1980**, *102*, 4790. (g) Kanno, T.; Oguchi, T.; Sakuragi, H.; Tokumaru, K.; Kobayashi, T. *Denki Kagaku* **1981**, *49*, 134. (h) Eberson, L. *Adv. Phys. Org. Chem.* **1982**, *18*, 79. (i) Masnovi, J. M.; Seddon, E. A.; Kochi, J. K. *Can. J. Chem.* **1984**, *62*, 2552. (j) Mochida, K.; Itani, A.; Yokoyama, M.; Tsuchiya, T.; Worley, S. D.; Kochi, J. K. *Bull. Chem. Soc. Jpn.* **1985**, *58*, 2149. (k) Colonna, M.; Greci, L.; Poloni, M.; Marrosu, G.; Trazza, A.; Colonna, F. P.; Distefano, G. *J. Chem. Soc., Perkin Trans. 2* **1986**, 1229. (l) Anxolabehere, E.; Hapiot, P.; Savéant, J.-M. *J. Electroanal. Chem.* **1990**, *282*, 275. (m) Nau, W. M.; Adam, W.; Klapstein, D.; Sahin, C.; Walter, H. *J. Org. Chem.* **1997**, *62*, 5128.

(19) Lias, S. G. Ionization Energy Evaluation. In *NIST Chemistry WebBook, NIST Standard Reference Database Number 69*; Linstrom, P. J., Mallard, W. G., Eds.; National Institute of Standards and Technology: Gaithersburg, MD, http://webbook.nist.gov. See the Supporting Information for ionization potential values.

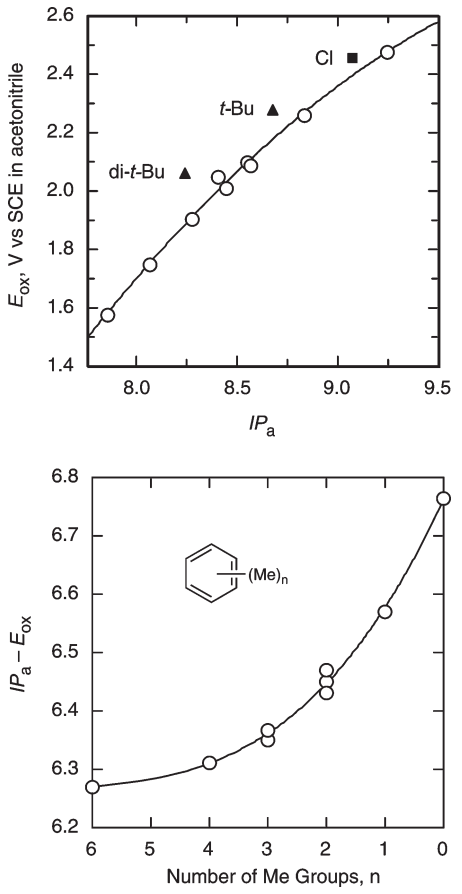

FIGURE 9. (Top) Plot of oxidation potentials for benzene and methyl-substituted benzenes (circles), *tert*-butyl-substituted benzenes (triangles), and chlorobenzene (square) in acetonitrile vs their adiabatic ionization potentials (IP_a). (Bottom) Plot of $IP_a - E_{ox}$ for methyl-substituted benzenes. Interpolated lines are drawn through the circles.

its methyl-substituted derivatives (circles) shows distinct downward curvature, demonstrating a nonlinear increase in stabilization of the radical cations by the solvent (acetonitrile) as the benzenes are decreasingly substituted. This trend is more clearly illustrated in the bottom part of Figure 9, where a plot of $(IP_a - E_{ox})$ vs number of methyl groups shows that the difference in solvation energies is nearly 0.5 eV greater for benzene than hexamethylbenzene. These results can be explained by decreased solvation with methyl substitution caused by increased charge delocalization[5k,20] and steric effects. Charge delocalization presumably also plays a role in the difference of $(IP_a - E_{ox})$ between naphthalene (6.36 eV)[21] and benzene (6.76 eV). The 0.4 eV energy difference reflects the decrease in solvent stabilization for oxidation of two-ring vs one-ring compounds in acetonitrile. This effect extends to biphenyl, which has $(IP_a - E_{ox}) = 6.21 \pm 0.13$ eV, comparable to that of naphthalene. It is apparent from the data in Figure 9 that the lower solvation energies associated with oxidation of these two-ring compounds is comparable to the effect of four to six methyl groups on the benzene ring.

As shown in the top of Figure 9, *tert*-butylbenzene (B3) and 1,4-di-*tert*-butylbenzene (B7) (triangles) both have higher oxidation potentials than the line through the methyl-substituted benzene data points, with the deviation being twice as large for B7 (0.14 V) as for B3 (0.07 V). These results can be attributed to steric inhibition of solvation of the radical cations of the *tert*-butyl derivatives. Interestingly, E_{ox} for chlorobenzene (B2) also shows a positive deviation of 0.03 V relative to the methyl-substituted benzenes. As the steric size of a chlorine substituent is smaller than a methyl group,[22] this result demonstrates that the nature of the substituents, not simply their size and number, can also play a role in the differential solvent stabilization of radical cations.

The biphenyl derivatives for which oxidation potentials were determined in this study contain a range of electron-donating and electron-withdrawing substituents. This provided an opportunity to determine if the oxidation potentials could be correlated with Hammett-type substituent constants. Prior correlations between oxidation potentials and Hammett/Brown σ^+ values[23] have been observed for a variety of electron donors, including triarylamines,[24] aryl sulfides, selenides and tellurides,[25] vinyl ethers and thioethers,[26] styrenes,[27] and arylmethyl radicals.[28] As shown in Figure 10, there is an excellent correlation between E_{ox} and the sum of the σ^+ values for the biphenyl derivatives, which should be helpful in estimating oxidation potentials of other biphenyl derivatives. Not surprisingly, the dependence of E_{ox} on $\Sigma\sigma^+$ is quite strong, with a slope of 9.0 kcal/mol, which is equivalent to $\rho = -6.7$.

It is worth noting that the higher E_{ox} values of *tert*-butylbenzene and 1,4-di-*tert*-butylbenzene relative to toluene and *p*-xylene discussed above are consistent with the less negative σ_p^+ value of a *tert*-butyl group (−0.26) compared to a methyl group (−0.31).[23] However, that the methyl derivatives have *higher* adiabatic ionization potentials reveals that the lower oxidation potentials of the methyl-substituted analogues is not simply due to the greater "electron-releasing" power of a methyl group, but rather due to the greater solvent-stabilization of cations that carry the smaller alkyl group. Solvation also plays a clear role in the reversal of the oxidation potentials for the pairs toluene (B4)/*tert*-butylbenzene(B3) and *p*-xylene(B10)/1,4-di-*tert*-butylbenzene(B7) in acetonitrile (Table 1) vs trifluoroacetic

(20) (a) Wayner, D. D. M.; Sim, B. A.; Dannenberg, J. J. *J. Org. Chem.* **1991**, *56*, 4853. (b) Jonsson, M.; Houmam, A.; Jocys, G; Wayner, D. D. M. *J. Chem. Soc., Perkin Trans. 2* **1999**, 425. (c) Svith, H.; Jensen, H.; Almstedt, J.; Andersson, P.; Lundbäck, T.; Daasbjerg, K; Jonsson, M. *J. Phys. Chem. A* **2004**, *108*, 4805.

(21) The equilibrium constants between the radical cations of naphthalene and durene as well as between naphthalene and 1,2,3,5-tetramethylbenzene in acetonitrile were determined previously to be 2.4 and 0.24, respectively (Gould, I. R.; Ege, D.; Moser, J. E.; Farid, S. *J. Am. Chem. Soc.* **1990**, *112*, 4290). Based on the oxidation potential of durene (1.75 V vs SCE) and 1,2,3,5-tetramethylbenzene (1.82 V) an oxidation potential of 1.78 ± 0.01 V is calculated for naphthalene.

(22) Meyer, A. *J. Chem. Soc., Perkin Trans. 2* **1986**, 1567.

(23) Hansch, C.; Leo, A.; Hoekman, D. *Exploring QSAR, Hydrophobic, Electronic and Steric Constants*; American Chemical Society: Washington, DC, 1995.

(24) Dapperheld, S.; Steckhan, E.; Brinkhus, K.-H. G.; Esch, T. *Chem. Ber.* **1991**, *124*, 2557.

(25) Engman, L.; Persson, J.; Andersson, C. M.; Bergulnd, M. *J. Chem. Soc., Perkin Trans. 2* **1992**, 1309.

(26) Bauld, N. L.; Alpin, J. T.; Yueh, W.; Endo, S.; Loving, A. *J. Phys. Org. Chem.* **1998**, *11*, 15.

(27) Che, C.-M.; Li, C.-K.; Tang, W.-T.; Yu, W.-Y. *J. Chem. Soc., Dalton Trans.* **1992**, 3153.

(28) Sim, B. A.; Milne, P. H.; Griller, D.; Wayner, D. D. M. *J. Am. Chem. Soc.* **1990**, *112*, 6635.

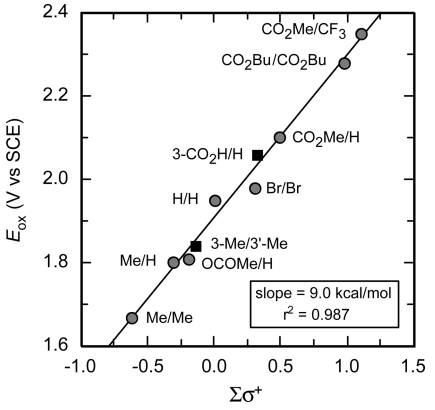

FIGURE 10. Plot of E_{ox} vs $\Sigma\sigma^+$ for the biphenyl derivatives. Biphenyls with meta (3 and 3′) substituents are indicated by squares and with para (4 and 4′) substituents by circles. σ^+ values[23] relative to the biphenyl are as follows: *p*-Me = −0.31, *m*-Me = −0.07, *p*-Br = 0.15, *p*-CO_2Me = 0.49, *p*-CO_2Bu = 0.49, *m*-CO_2H = 0.32, *p*-CF_3 = 0.61, and OCOMe = −0.19. Literature values for E_{ox} of 3,3' -dimethylbiphenyl and 4,4' -dimethylbiphenyl were used.[10]

acid. In acetonitrile, E_{ox}(B4) is less than E_{ox}(B3) by 0.02 V and E_{ox}(B10) is less than E_{ox}(B7) by 0.05 V (Table 1). In contrast, in CF_3CO_2H the relative oxidation potentials are reversed; with E_{ox}(B4) > E_{ox}(B3) by 0.08 V and E_{ox}(B10) > E_{ox}(B7) by 0.03 V.[5k] These data clearly demonstrate the risks of assuming the transferability of even relative oxidation potentials from one solvent to another. It is worth emphasizing that such a conclusion would be difficult to make with confidence in the absence of reliable oxidation potentials.

Additionally, with regard to solvation effects, the similarity of the oxidation potential differences between B7 and B10 in acetonitrile (dielectric constant = 36) and ethyl acetate (dielectric constant = 6) implies that solvent dielectric constant is not a major differentiating factor. The trend observed for the four solvents studied does suggest a possible correlation with solvent β, a measure of hydrogen bond accepting ability.[29] Reduced steric hindrance and/or positive charge localization on the methyl hydrogen atoms of B10 due to hyperconjugation may result in greater solvation stabilization in hydrogen bond accepting solvents such as acetonitrile and ethyl acetate. For the low-β solvents, the lowering of the relative E_{ox} of B10 in methylene chloride (n = 1.424) compared to trifluoroacetic acid (n = 1.285) suggests that radical cations with greater positive charge localization may also undergo greater solvation stabilization in higher polarizability solvents.

4. Conclusion

Accurate oxidation potentials have been determined in acetonitrile for a large number of biphenyl and benzene derivatives, including benzene and toluene, which have not been possible to measure by electrochemical methods. The oxidation potentials were determined by measuring equilibrium constants for electron exchange between neutral electron donors and their corresponding radical cations using several nanosecond transient absorption methods. While electron-exchange equilibrium could be directly observed in some cases, kinetic methods were found to be complementary when either ΔE_{ox} between the substrates undergoing electron transfer was too large or when dimer radical cation formation complicated the equilibrium processes. Equilibrium constants for dimer radical cation formation were also determined, as well as aborption maxima and extinction coefficients for the radical cations studied.

The increase in the oxidation potentials of benzene derivatives with decreasing alkyl substitution was found to be smaller than the corresponding increase in their gas phase ionization potentials. This result is consistent with increasing solvent stabilization of radical cations with decreasing alkyl substitution on the benzene ring. In addition, differential solvent effects were found to lead to reversal of relative oxidation potentials in several cases.

The transient absorption methods described herein should be of general use for the determination of thermodynamically meaningful oxidation potentials. These, in turn, will be valuable for critically testing a variety of thermodynamic and thermokinetic correlations. Further work along these lines is in progress.

Experimental Section

Materials. Acetonitrile (99.93+% Baker, HPLC grade, 5 ppm H_2O), trifluoroacetic anhydride (>99%), trifluoroacetic acid (99.5+%), methylene chloride (99.9+%), and ethyl acetate (99.8+%) were used as received. *N*-Methylquinolinium hexafluorophosphate (NMQ^+)[10] was recrystallized from methanol. Solid benzene and biphenyl derivatives were purified by recrystallization. Most liquids were fractionally distilled. Some high-purity benzene derivatives were on hand, including 99.99% toluene (EMD OmniSolv) and vacuum-sealed ampules formerly available from the American Petroleum Institute. Particular care was taken to purify benzene because traces of toluene or other more easily oxidized derivatives could competitively form radical cations under experimental conditions. Benzene (99.96%, EMD OmniSolv) was first purified by several cycles of partial (~80%) freezing with removal of the unfrozen liquid, followed by fractional distillation from calcium hydride. The resulting material contained ≤1 ppm of toluene and other benzene derivatives as determined by gas chromatographic analysis.

Biphenyl derivatives were commercially available except for *n*-butyl 4′-(trifluoromethyl)biphenyl-4-carboxylate (BP1), which was prepared as described below.

Synthesis of 4′-Trifluoromethylbiphenyl-4-carboxylic Acid. A mixture of 1.35 g of 4′-carboxyphenylboronic acid (8.13 mmol), 0.12 g of triphenylphospine (0.47 mmol), 1.1 mL of 4′-bromobenzotrifluoride (7.75 mmol), 0.0345 g of palladium acetate (0.16 mmol), and 1.6 g of sodium carbonate (15.5 mmol) in 30 mL of a 1:1 acetone/water was refluxed under a nitrogen atmosphere for 5 h. After being cooled to room temperature, the reaction mixture was filtered through a pad of silica gel and partially concentrated in vacuo. The residue was filtered to remove palladium black, and the filtrate was acidified with HCl. The resulting white solid was collected, washed with water, and dried (1.84 g, 89%). The crude product was used without further purification: ^{1}H NMR (500 MHz DMSO-d_6) δ 13.08 (br, 1.0 H), 8.07 (d, J=15 Hz, 2.1 H), 7.98 (d, J=12.5 Hz, 1.9 H), 7.87 (d, 2.0 H), 7.85 (d, 2.0 H).[30]

Synthesis of *n*-Butyl 4′-(Trifluoromethyl)biphenyl-4-carboxylate (BP1). A mixture of 1.84 g of 4′-trifluoromethylbiphenyl-4-carboxylic acid, 30 mL of *n*-butanol, 0.5 mL of sulfuric acid,

(29) Kamlet, M. J.; Abboud, J-L. M.; Abraham, M. H.; Taft, R. W. *J. Org. Chem.* **1983**, *48*, 2887 (β values: ethyl acetate = 0.45; acetonitrile = 0.31; methylene chloride = 0.0; trifluoroacetic acid ~ 0.0).

(30) Korolev, D. N.; Bumagin, N. A. *Tetrahedron Lett.* **2005**, *46*, 5751.

and 3 Å molecular sieves was refluxed under a nitrogen atmosphere for 16 h. The mixture was filtered while hot, and the sieves were rinsed with diethyl ether. The filtrate was successively washed with water and 5% aq $NaHCO_3$, dried over anhydrous $MgSO_4$, and concentrated in vacuo to give a pale yellow solid. Purification by column chromatography (SiO_2, 99:1 hexanes/EtOAc) followed by two recrystallizations from 3:1 2-propanol/water gave white plates (0.87 g, 35%; mp 54−55 °C): ^{1}H NMR (400 MHz $CDCl_3$) δ 8.20 (d, J=4.2 Hz, 1.9 H), 7.78 (s, 3.9 H), 7.72 (d, J = 4 Hz, 2.0 H), 4.42 (t, J=6.8 Hz, 2.0 H), 1.85 (quin, 2.1 H), 1.57 (sext, 2.0 H), 1.06 (t, J = 8.2 Hz, 3.0 H); ^{13}C NMR (125 MHz $CDCl_3$, with assignments based on DEPT-135 and HSQC spectra, and a gated decoupling experiment to obtain accurate peak integrals) δ 166.3 (C=O), 143.9 (C1 or C1′), 143.6 (C1 or C1′), 130.2 (C3/5 + C4), 130.1 (C4′, q, J_{CF} = 32.4 Hz), 127.6 (C2′/6′), 127.2 (C2/6), 125.8 (C3′/5′, q, J_{CF} = 3.5 Hz), 124.15 (CF_3, q, J_{CF} = 270 Hz), [65.01, 30.8, 19.3, 13.8, $CH_2CH_2CH_2CH_3$]. Anal. Calcd for $C_{18}H_{17}F_3O_2$: C, 67.07; H, 5.32. Found: C, 67.04; H, 5.28.

Laser Flash Photolysis Measurements. Radical cation absorption spectra and transient kinetics measurements were performed using a nanosecond laser flash photolysis apparatus. A Lambda Physik Lextra 50 XeCl excimer laser was used to pump a Lambda Physik 3002 dye laser, providing approximately 7 ns pulses with an energy of about 2 mJ. Most measurements were carried out using 343 nm excitation obtained with *p*-terphenyl as the laser dye. Transient absorptions were monitored at 90° to the laser excitation using pulsed xenon lamps, timing shutters, a monochromator, and a photomultiplier tube for kinetic measurements or a diode array detector for obtaining transient absorption spectra. For kinetic analyses the signal from the photomultiplier tube was directed into a Tektronix TDS 620 digitizing oscilloscope and then to a computer for viewing, storage, and analysis. Beam energies were typically attenuated to less than 1 mJ per pulse to reduce second order radical ion decay and minimize photodegradation. Data were averaged over 20−40 pulses and experiments were carried out at ambient temperature (~295 K).

In addition to the electron donors whose radical cation equilibria were to be measured, solutions usually contained 1 mM NMQ^+ sensitizer along with 0.5 M toluene in air-saturated acetonitrile. For the measurement of E_{ox} values of toluene and electron donors with higher or slightly lower E_{ox} values, a codonor was not used, and donor concentrations were selected that were sufficiently high for rapid electron transfer to $^1NMQ^+$*.

The energy of $^1NMQ^+$* was estimated to be 3.53 eV from the intersection of absorption and fluorescence spectra. A laser photolysis equilibration procedure was used to determine the reduction potential for NMQ^+ in acetonitrile (−0.91 V vs SCE).[31] Thus, the reduction potential of $^1NMQ^+$* is ~2.62 V vs SCE, sufficient to oxidize all donors used in this study, including benzene.

In some cases, small amounts (0.5−1.0% by volume) of trifluoroacetic anhydride were added to solutions to scavenge traces of water that could otherwise decrease radical cation lifetimes. This resulted in significant lifetime increases (e.g., to 25 μs) for many radical cations and greatly simplified some equilibrium and kinetic measurements. Minimal lifetime changes with added trifluoroacetic anhydride were observed for benzene and toluene radical cations whose decay may be controlled by reaction with solvent and return electron transfer from superoxide. It was also found that addition of small amounts (~1.0% by volume) of trifluoroacetic acid produced similar increases in the radical cation lifetimes and their decays became strictly first order, even at relatively high laser powers. This observation may be due to protonation of $O_2^{\bullet-}$ under these conditions, thus reducing second-order return-electron transfer. Radical ion decay is further discussed in the Supporting Information.

Acknowledgment. Research was supported by a grant from the National Science Foundation (CHE-0749919).

Supporting Information Available: Benzene radical cation absorption spectra as a function of [benzene]; analysis of radical cation equilibria; fitting of spectra of equilibrated radical cations; K_{eq} relationship ladder showing the pairwise comparisons used to obtain E_{ox} values; ionization potentials; rate constants for radical decay. ^{1}H and ^{13}C NMR spectra of BP1. This material is available free of charge via the Internet at http://pubs.acs.org.

(31) Merkel, P. B.; Luo, P.; Dinnocenzo, J. P.; Farid, S. Manuscript in preparation.